REPORT DOCUMENTATION PAGE

Form Approved OMB No. 0704-0188

1. REPORT DATE *(DD-MM-YYYY)*	2. REPORT TYPE	3. DATES COVERED *(From – To)*
28-02-2002	Final Report	22 September 2000 - 22-Nov-01

4. TITLE AND SUBTITLE

The Effects of LCF Loadings on HCF Crack Growth--Phase IV

5a. CONTRACT NUMBER
F61775-00-WE041

5b. GRANT NUMBER

5c. PROGRAM ELEMENT NUMBER

6. AUTHOR(S)

R.F. Hall, B.E. Powell and J. Byrne

5d. PROJECT NUMBER

5d. TASK NUMBER

5e. WORK UNIT NUMBER

7. PERFORMING ORGANIZATION NAME(S) AND ADDRESS(ES)

University of Portsmouth
Anglesea Building, Anglesea Road
Portsmouth PO1 3DJ
United Kingdom

8. PERFORMING ORGANIZATION REPORT NUMBER

N/A

9. SPONSORING/MONITORING AGENCY NAME(S) AND ADDRESS(ES)

EOARD
PSC 802 BOX 14
FPO 09499-0014

10. SPONSOR/MONITOR'S ACRONYM(S)

11. SPONSOR/MONITOR'S REPORT NUMBER(S)
SPC 00-4041

12. DISTRIBUTION/AVAILABILITY STATEMENT

Approved for public release; distribution is unlimited.

13. SUPPLEMENTARY NOTES

14. ABSTRACT

This report results from a contract tasking University of Portsmouth as follows: The contractor will investigate high cycle fatigue (HCF) effects in structural materials. This work will be a logical follow-on to three previous phases conducted under EOARD contract. In this phase, the contractor will: 1) extend the study of the effect of prior overloads by the employment of larger overload ratios; 2) establish the conditions at which the effects of overloads in the HCF + LCF loadings completely suppress the damage caused by HCF cycles; and 3) extend the analysis of new models to overcome the shortcomings of the Wheeler model to predict the onset of HCF cycle damage.

15. SUBJECT TERMS
EOARD, Materials, Metals & alloys, Fatigue

16. SECURITY CLASSIFICATION OF:			17. LIMITATION OF ABSTRACT	18, NUMBER OF PAGES	19a. NAME OF RESPONSIBLE PERSON
a. REPORT	b. ABSTRACT	c. THIS PAGE			Charles H. Ward, Lt Col, USAF
UNCLAS	UNCLAS	UNCLAS	UL	34	**19b. TELEPHONE NUMBER** *(Include area code)* +44 (0)20 7514 3154

UNIVERSITY OF PORTSMOUTH

US AFOSR Study Report

The effects of LCF loadings on HCF crack growth

Final Report for Phase IV

F571

Submitted by:

R.F. Hall, B.E. Powell and J.Byrne

February 2002

MECHANICAL BEHAVIOUR OF MATERIALS LABORATORY

DEPARTMENT OF MECHANICAL AND MANUFACTURING ENGINEERING

Anglesea Building, Anglesea Road
Portsmouth PO1 3DJ

Phone: +44 (0)23 92 842370 E-mail: jim.byrne@port.ac.uk
Phone: +44 (0)23 92 842325 E-mail: rod.hall@port.ac.uk
Fax: +44 (0)23 92 842351

THE EFFECT OF LCF LOADINGS ON HCF CRACK GROWTH

REPORT FOR THE PERIOD to February 2002

REPORT NO F 571

NOTATION

CN	corner notched
DCPD	direct current potential difference
FCG	fatigue crack growth
FOD	foreign object damage
HCF	high cycle fatigue
LCF	low cycle fatigue
MOC	multiple overload cycles: a type of HCF + LCF loading
MUC	multiple underload cycles: a type of HCF + LCF loading
SOC	single overload cycle: a type of HCF + LCF loading
SUC	single underload cycle: a type of HCF + LCF loading
da/dN_{HCF}	crack growth increment resulting from the application of a HCF cycle
da/dN_{LCF}	crack growth increment resulting from the application of a LCF cycle
da/dB	crack growth increment resulting from the application of a HCF + LCF loading block
da/dB_{HCF}	crack growth increment resulting from the application of the HCF cycles within a loading block
da/dB_{LCF}	crack growth increment resulting from the application of the LCF cycles within a loading block
ΔK, DK	stress intensity range
ΔK_{HCF}	stress intensity range associated with a HCF cycle
ΔK_{LCF}	stress intensity range associated with a LCF cycle, i.e. the peak-to-peak load cycle
$\Delta K_{HCF.onset}$	the value of ΔK_{HCF} associated with the onset of HCF crack growth
$\Delta K_{LCF.onset}$	the value of ΔK_{LCF} associated with the onset of HCF crack growth
ΔK_{th}	threshold value of stress intensity range
$K_{max.th}$	threshold value of maximum stress intensity
$\sigma_{max,HCF}$	maximum HCF stress
$\sigma_{min,HCF}$	minimum HCF stress
$\sigma_{max,LCF}$	maximum LCF stress
$\sigma_{min,LCF}$	minimum LCF stress
N_{HCF}	number of HCF cycles in a loading block
N_{LCF}	number of LCF cycles in a loading block
n	ratio N_{HCF} : N_{LCF}
R_{HCF}	stress ratio of the HCF cycles
R_{LCF}	stress ratio of the LCF cycles
s	seconds
T	overload ratio; i.e. the maximum LCF stress / maximum HCF stress.
W	Wheeler constant

INTRODUCTION

A current design limitation for aero-engine discs and fan blades is that of the material's resistance to low cycle fatigue (LCF). In such rotating components the LCF loading arises from the cyclic variation of both the centrifugal and the thermal stresses. In the simplest case this substantial stress variation occurs once per flight. However, rotating engine components may also experience high cycle fatigue (HCF) failures as a direct result of excessive vibrational stresses. Consequently, in order that the fatigue integrity of these critical rotating components might be fully assessed, it is necessary to establish the resistance of the disc or fan blade material to the conjoint action of HCF and LCF loadings.

The present work is concerned to measure and model the fatigue crack growth (FCG) rates associated with HCF loadings, particularly as they are affected by the presence of different proportions of LCF induced fatigue crack growth. The threshold values for HCF crack growth, both in the presence and absence of LCF crack growth, are studied, since they may be used to calculate critical crack sizes for components and structures subjected to HCF stress cycles.

Corner notched specimens of forged Ti-6Al-4V have been cyclically loaded in a special test facility which combines an electromagnetic vibrator with a servo-hydraulic fatigue machine. This hybrid machine can therefore apply HCF cycles and LCF cycles either separately or conjointly. The HCF cycles are of sinusoidal form and the LCF cycles are trapezoidal

A pulsed direct current potential difference (DCPD) system has been used to monitor crack growth. Voltage readings from the notch of the specimen and at a remote reference point have been measured by a multimeter with a resolution of 0.001mV and automatically downloaded onto a computer spreadsheet. Analysis of the test results is

presented as diagrams of FCG rate, da/dN, by the 3-point secant method, against ΔK calculated using Pickard's **[1]** solution for CN type specimens.

When HCF and LCF cycles are conjointly applied, initially at low values of ΔK, the HCF cycles are not effective. However, at a value of ΔK dependent on factors such as material being tested and load levels of both LCF and HCF cycles, the HCF cycles commence to contribute to the overall FCG rate. With a large number of HCF cycles compared to LCF cycles, this point usually signifies the end of useful life. The effect is schematically presented in Figure **1**, where ΔK_{onset} is the point at which the HCF cycles become effective.

The tests which are covered in this report have involved a cyclic regime which more closely resembles the flight pattern of aircraft than the simple HCF cycles at constant load amplitudes in one LCF cycle which have been described on in past reports **[2, 3, 4, & 5]**. A schematic representation of the waveform based on information supplied by Rolls-Royce, is given in Figure **2**. The stress induced in the specimen rose to a high mean level from a minimum load of zero, under the application of the LCF load. Initially HCF cycles of large amplitude were applied to simulate the stresses encountered in an aero-engine during aircraft TAKE-OFF. After relatively few cycles, both the mean stress and the amplitude of the HCF cycles were reduced, to a representation of the climbing stage of aircraft flight. In reality the stresses on aero-engines are constantly altering during climbing due to changes in air density with altitude. As a simplification for experimentation, the climbing was divided into three stages and each stage had constant stress levels. The second and third stages of climb had reduced HCF amplitude with slightly increased mean stress but the maximum stress being reduced stage by stage. The mean stress and HCF amplitude were further reduced for the CRUISE stage of flight with 7000 000 HCF cycles applied. On completion, the HCF cycles ceased, the load reduced to zero and then reapplied to the mean stress level for TAKE-OFF stage. The removal and reapplying of the LCF load has the designation of the STOP\START stage.

Because the maximum stress is reduced at each stage of the flight simulation, all the CLIMB stages and the CRUISE stage have in effect LCF overload imposed by the previous stage. The amplitude of the overload is signified by the value of 'T' (present maximum stress/immediate past maximum stress) in Figure **2,** where T=1.0 indicates no overload. Also given in Figure **2** are the maximum and minimum stresses at each stage, the number of HCF cycles applied during each stage and the HCF stress ratio.

Because of the different HCF stresses for each stage of the flight simulation, each stage has a different value of ΔK_{onset}, with the consequence that one stage will commence to contribute to FCG, then as the crack extends, increasing the value of ΔK, other stages progressively become active. With the largest stress range at the TAKE-OFF stage, it is to be expected that the HCF cycles of this stage would be the first to contribute to FCG. Once each ΔK_{onset} has been exceeded, the number of HCF cycles applied will greatly influence the impact that stage has on overall crack growth.

Before the start of testing, the crack in the test specimen was grown, by applying LCF cycles only, to a length just short of that at which the first HCF cycles were expected to become active. This was to reduce the time taken for testing to a reasonable length by eliminating much unproductive HCF cycling. Thus the ΔK just at the start of testing was just below onset for TAKE-OFF.

During the test, values of the DCPD voltages were recorded when the HCF cycles commenced and finished, and at each change in amplitude. From these voltages the average crack growth by each stage of the flight could be determined and it was hoped that the onset of the HCF cycles at each stage of the flight simulation could be found.

The test was terminated when the crack length exceeded half the specimen width. This also happened to be at the approximate point when the application of one further flight simulation would result in specimen fracture before it could be completed.

2. RESULTS

Two separate flight simulation tests were completed and the results are presented as two sets of diagrams, one set for each test. Also presented in this report are diagrams of near-threshold FCG rates for the three stress ratios used in the overload tests in earlier phases of the test programme. At least two tests for each stress ratio were completed.

Figures **3** and **4** present the crack extension produced by each stage of each flight simulation. The first flight simulation where crack growth due HCF cycles was detected has been designated flight number 1. The number of flight simulations where crack growth was solely produced by LCF cycles (STOP\START stage) was not recorded. Each column in Figures **3** and **4** represent one flight simulation, and the contribution from each stage is depicted in a different colour. Starting at around 0.75mm, the prior crack length for subsequent columns has the addition of all HCF crack growth of the previous cycle.

In both Figures **3** and **4** it can be seen that the STOP\START stage continues to contribute to crack growth but HCF cycles contribute an increasing amount to that growth. However in the early stages of HCF crack growth the FCG rate is small and difficult to resolve in the scatter in DCPD readings with the result that it is not possible to establish whether the TAKE-OFF or the CLIMB 1 stage contributed first to crack growth. In both tests when the FCG rates of the TAKE-OFF and CLIMB 1 become

discernible it is the greater number of HCF cycles in the CLIMB 1 stage that cause the greater increase in crack extension.

As expected, the CLIMB 2 stage contributes later to the overall FCG rate and results from test 1 would indicate CLIMB 3 follows. It would appear from test 1 that ΔK_{onset} for the CRUISE stage HCF cycles had not been reached, but from test 2 it is seen that after onset, the large number of HCF cycles in the CRUISE stage is significant. The test was stopped after just over 500 000 of the 700 000 HCF cycles intended for the CRUISE stage because of the rapidly extending crack. This emphasises the contention that where large numbers of HCF cycles are involved, the onset of HCF crack growth effectively signals the end of useful life.

The data for crack extension per flight are presented as 'a-N' type diagrams in Figures **5** and **6**. Some variation in FCG between each flight is evident within the general trend of increasing crack growth as the crack lengthens. The rapidly increasing crack growth rate of all stages towards the end of the tests is again clearly demonstrated.

Each stage of both tests was then analysed by plotting the crack extension per HCF cycle against the value of ΔK calculated using the crack length at the end of the stage for individual flight simulations, Figures **7** to **12** being the result. A polynomial curve has been fitted to each set of data, which has been used subsequently to represent that data in analyses and in comparisons with other data. The curve has been visually fitted. In the experimental data from the TAKE-OFF and first two stages of CLIMB, there is a small

amount of scatter and relatively large FCG rates (maximum around 10^{-5} mm/cycle), Figures **7**, **8** and **9**. The FCG rates for CLIMB 3 stage, Figures **10a** and **10b**, are much closer to threshold and at these small increases of crack length, scatter can be a large factor in the data. Scatter inherent in the DCPD readings starts to become significant at the small changes in voltage ratio from which these FCG rates are calculated. However the relatively consistency of the data inspires some confidence in it's integrity.

Apart from the final flight in test 2, the FCG rates in the CRUISE stage, Figures**11a** & **11b**, all fall below the accepted value for threshold (10^{-8}mm/cycle) which makes them unreliable. There is also a large scatter in the results, relative to the data from the other stages. In addition, from test 1 the CRUISE stage data from only 4 flight simulations could be used, Figure **11a**, because the DCPD readings from the other sets of data suggested either an extremely small FCG rate, or a negative change in crack length which is clearly impossible. No attempt has been made, therefore, to represent the growth rate data for the CRUISE stage by a polynomial curve.

Data from the STOP\START stage, Figures **12a** and **12b** exhibit larger FCG rates than the HCF cycles, as expected. The exceptional FCG rates in Figures **12a** and **12b** are caused by problems with the testing machine when several STOP\START stages had to be applied before normal cycling could be attained in the subsequent flight simulation. These anomalies have been ignored in the construction of the polynomial curve.

Flight diagrams of crack growth per stage have been reconstructed by summing the crack extensions for each stage using the experimental values of ΔK with the polynomial curve to calculate the crack growth per HCF cycle and then multiplying by the number of cycles for that stage. Thus experimental scatter in the data has been removed. Figures **13** and **14** demonstrate the difference between the experimental and reconstructed crack lengths that the use of the polynomial curves make in analysis of FCG data. The exception of the CRUISE stage at the end of the final flight, Figure **14**, should be noted. With the inability to calculate a crack extension value because of the absence of a polynomial curve for the CRUISE stage, in this single instance the experimental crack extension has been used.

Near-threshold FCG rates for HCF cycles at stress ratios of R_{HCF} = 0.7, 0.8 and 0.9 have been determined and are presented as Figures **15**, **16** and **17**. A diagram for R_{HCF}=0.8 has been presented previously **[2]** but the polynomial curve to the data has been amended. Threshold values determined previously by the jump-in method **[4]** have been incorporated in the diagrams and the polynomial curves, used to represent the experimental results, have been constructed through them.

Table 1 Values of ΔK_{th} determined by experimental jump-in method **[4]** used in Figures 15 to 17.

Stress Ratio R_{HCF}	**ΔK_{th} (MPa$\sqrt{m}$)**
0.7	3.0
0.8	2.4
0.9	2.0

Calculating the HCF stress ratio of each stage, results in the values stated in Figure **2.** With near-threshold FCG data for R_{HCF} = 0.8 and 0.9 available, Figures **16** and **17,** it is not unreasonable to compare the FCG rates for near-threshold at R_{HCF} =0.8 with the FCG rates for TAKE-OFF and CLIMB 1 which are R_{HCF} =0.82 and the FCG rates of near-threshold at 0.9 with the FCG rates for CLIMB 2 and CRUISE which are R_{HCF} = 0.88 and 0.903 respectively. The nearest near-threshold data to the CLIMB 3 stage at R_{HCF} =0.95 is at R_{HCF} =0.9.

Figure **18** illustrates the HCF data in the region of R_{HCF} =0.8. Above a stress intensity range of 4MPa$\sqrt{m}$ the flight simulation results compare closely to the near-threshold data. Below a stress intensity range of 3.5MPa$\sqrt{m}$ the flight simulation FCG rates appear to be delayed and suggest an FCG rate of 10^{-8} mm/cycle at around ΔK_{th} =3MPa$\sqrt{m}$. This suggests that threshold and thus HCF damage is retarded under flight conditions. At R_{HCF}=0.82 some increase over the value of ΔK_{th} at R_{HCF}=0.8 would be expected, but the increase is larger than could reasonably be expected from this cause because 3MPa$\sqrt{m}$ is the value of ΔK_{th} for R_{HCF} =0.7 **[Table 1].**

The CLIMB 2 stage of the two flight simulation tests, Figure **19** again indicates good correlation between the near-threshold HCF data and the FCG rates from the flight simulations, including low values of FCG rates approaching threshold. Thus there appears to be no retardation in the HCF cycles in the flight simulation. As explained above, no reliable data was obtained for the CRUISE stage of flight simulations, which is the reason for its omission in Figure **19.**

There is little correlation between the FCG rates from the CLIMB 3 stage of the flight simulations and the near-threshold FCG rates, Figure **20**, but as in Figures **18** and **19** the sets of data from the two flight simulation tests agree closely with each other. The large difference in FCG data is at least partly due to the difference in stress ratio, the value of ΔK_{th} at R_{HCF} =0.95 will be significantly less that that for R_{HCF} =0.9, given the reduction in ΔK_{th} from R_{HCF} =0.7 to R_{HCF} =0.9.

The crack growth during flight simulation was generally as expected and followed a well-established pattern except the CRUISE stage in which the results are inconsistent. The onset of each stage was generally as expected with the exception that no conclusion could be made as to whether TAKE-OFF or CLIMB 1 contributed first to the overall crack growth.

Climb 2 stage also contributed significantly to the overall FCG but always to a lesser extent than TAKE-OFF and CLIMB 1. Climb 3 stage never contributed a significant amount to the FCG. The CRUISE stage is inconsistent, with an all-or-nothing effect. There may not be any detectable contribution to FCG, as in test 1, or when there is, the number of HCF cycles involved results in this stage contributing the greatest amount to FCG, as in test 2, effectively terminating the flight.

The polynomial curves for each stage of the two flight simulation tests are very similar, as may be observed in Figures 18 to 20, being within the scatter of the experimental results from the tests.

No retardation in the general HCF FCG rates has been noted in the flight simulation tests, only near threshold at R_{HCF}= 0.8. This is not unexpected because in the CLIMB 1 and CLIMB 2 stages the prior overload ratio is small. In the CRUISE stage where some noticeable retardation might be expected there is no reliable data to base conclusions on.

CONCLUSIONS

1. FCG rates of the HCF cycles in flight simulations have been compared to the near-threshold FCG rates.
   For the TAKE-OFF, CLIMB 1 and CLIMB 2 stages of the flight simulations the FCG rates compare closely to the near-threshold FCG rates.
   The CLIMB 3 stage of the flight simulation shows significantly larger FCG rates below 3MPa$\sqrt{m}$ to the closest near-threshold FCG data available.

2. The occasion on which crack growth occurred during the CRUISE stage, the number of HCF cycles involved ensured that a large contribution to overall crack growth was made which could result in terminating the life of a component.

3. Predictions of crack development for flight simulations have been made based on individual block crack growth rate relationships and predicts within 5%.

4. From the FCG data from two flight simulation tests, retardation of HCF FCG rates has been found only very close to threshold at a stress ratio of R_{HCF} = 0.8.

REFERENCES

[1] Pickard, A.C. "The application of 3-dimentional finite element methods to fracture mechanics and fatigue life predictions" EMAS, 1986..

[2] Hall, R.F., & Powell, B.E. US AFOSR Study Report; Annual Report for Phase II, **F567**, May 1999

[3] Hall, R.F., Powell, B.E. & Byrne, J. US AFOSR Study Report; Annual Report for Phase III, **F568**, November 1999

[4] Hall, R.F., Powell, B.E. & Byrne, J. US AFOSR Study Report; Annual Report for Phase III, **F569**, October 2000

[5] Hall, R.F., Powell, B.E. & Byrne, J. US AFOSR Study Report; Annual Report for Phase III, **F570**, May 2001

Figures

Figure 12. FCG rates from STOP\START stage of flight simulations, with fitted polynomial curve. Figure 12a, test 1. Figure 12b, test 2.

Figure 13. Comparison of crack length from experimental data against predictions based on polynomial curves for FCG during individual stages of the final 5 flights in test 1.

Figure 14. Comparison of crack length from experimental data against predictions based on polynomial curves for FCG during individual stages of the final 5 flights in test 2.

Figure 15. Near-threshold FCG rates for HCF cycles at $R_{HCF} = 0.7$. Results from 2 tests.

Figure 16. Near-threshold FCG rates for HCF cycles at $R_{HCF} = 0.8$. Results from 2 tests.

Figure 17. Near-threshold FCG rates for HCF cycles at $R_{HCF} = 0.9$. Results from 2 tests.

Figure 18. Comparison of FCG rates for basic HCF data for near-threshold with TAKE-OFF and CLIMB 1 stages of flight simulations.

Figure 19. Comparison of FCG rates for basic HCF data for near-threshold with CLIMB 2 stage of flight simulations.

Figure 20. Comparison of FCG rates for basic HCF data for near-threshold with and CLIMB 3 stages of flight simulations.

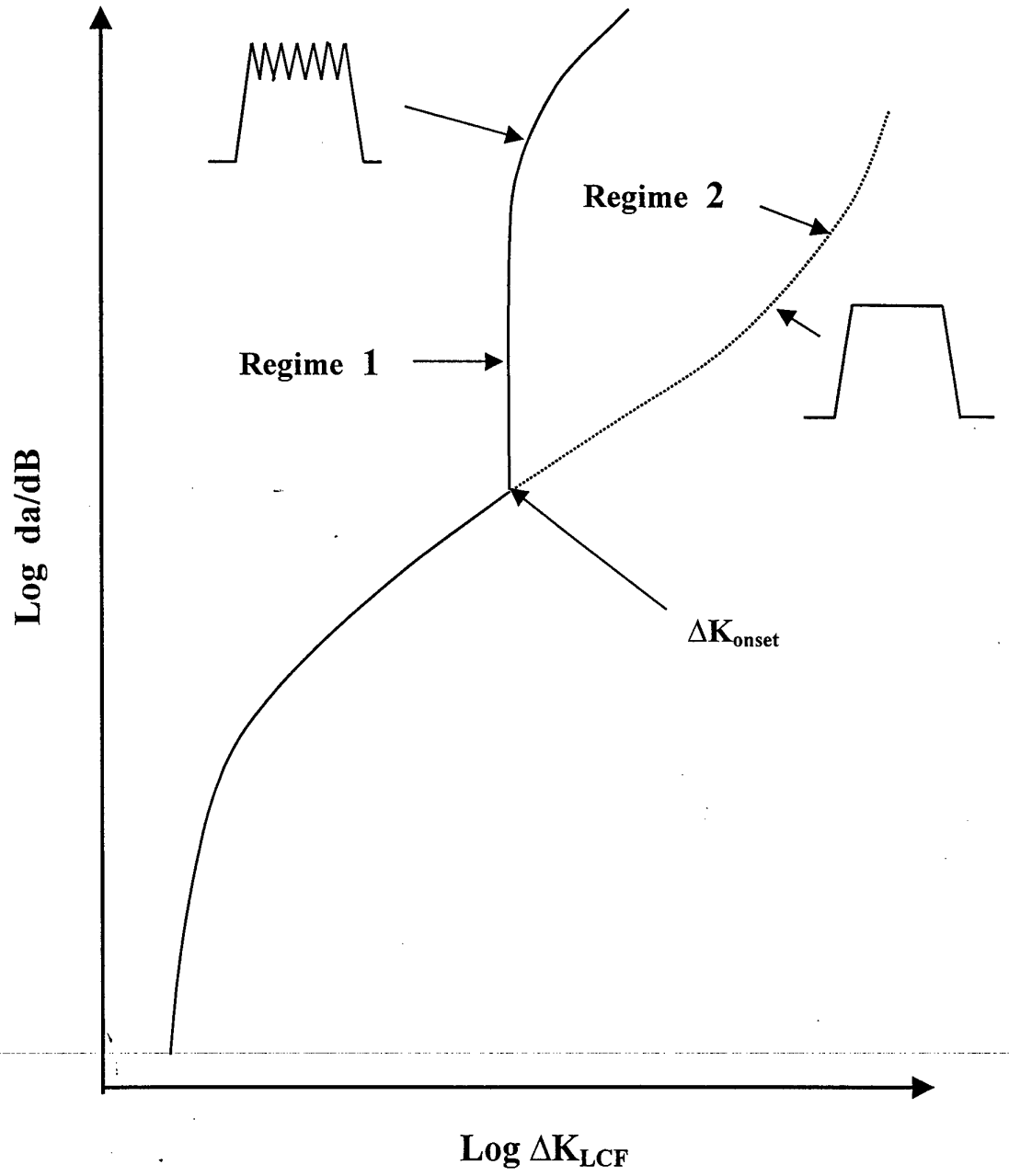

Figure 1 Form of fatigue crack growth rate curve for a simple HCF/LCF loading combination

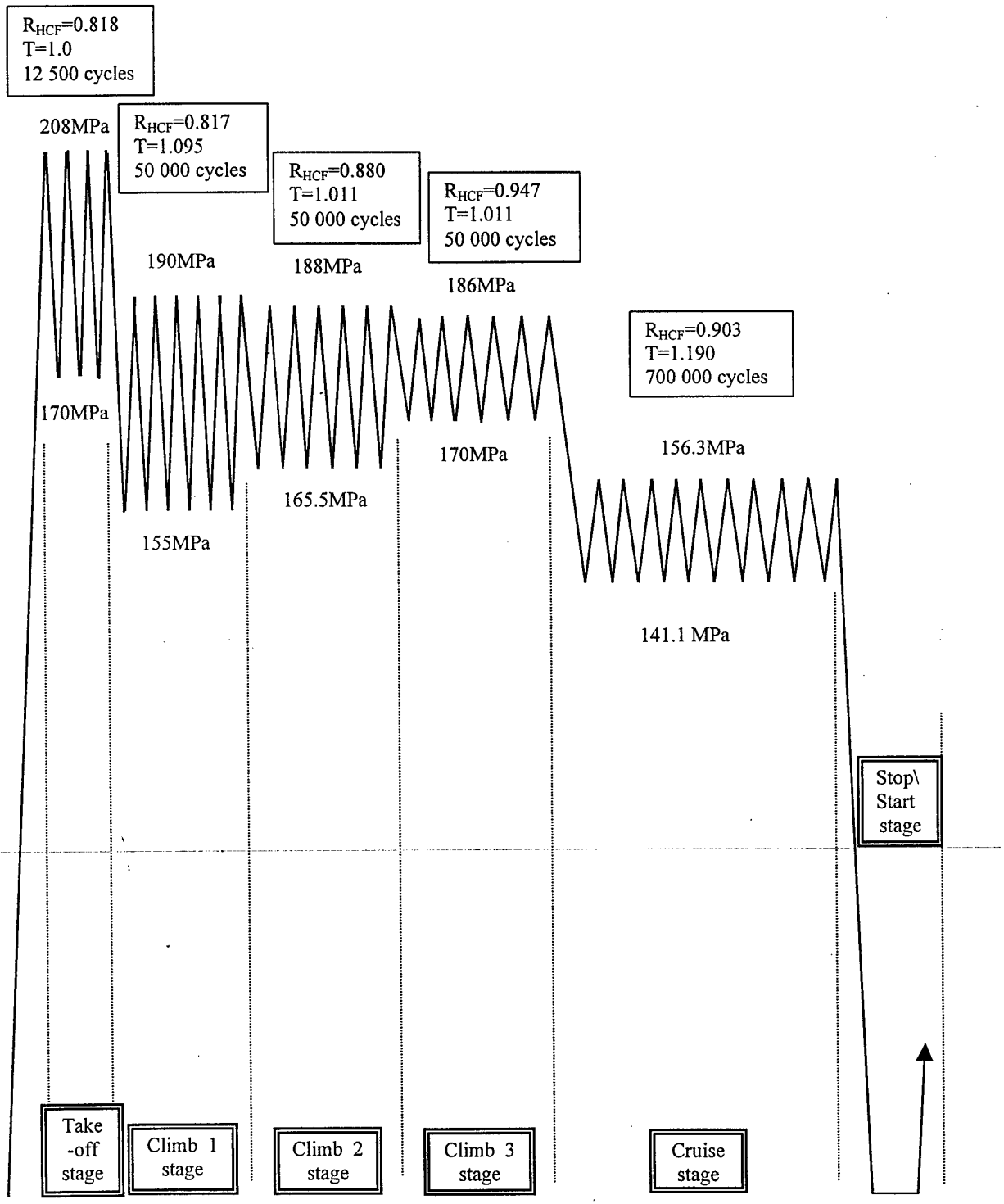

Figure 2 Schematic diagram of the stresses used in the Flight Simulation experiments.

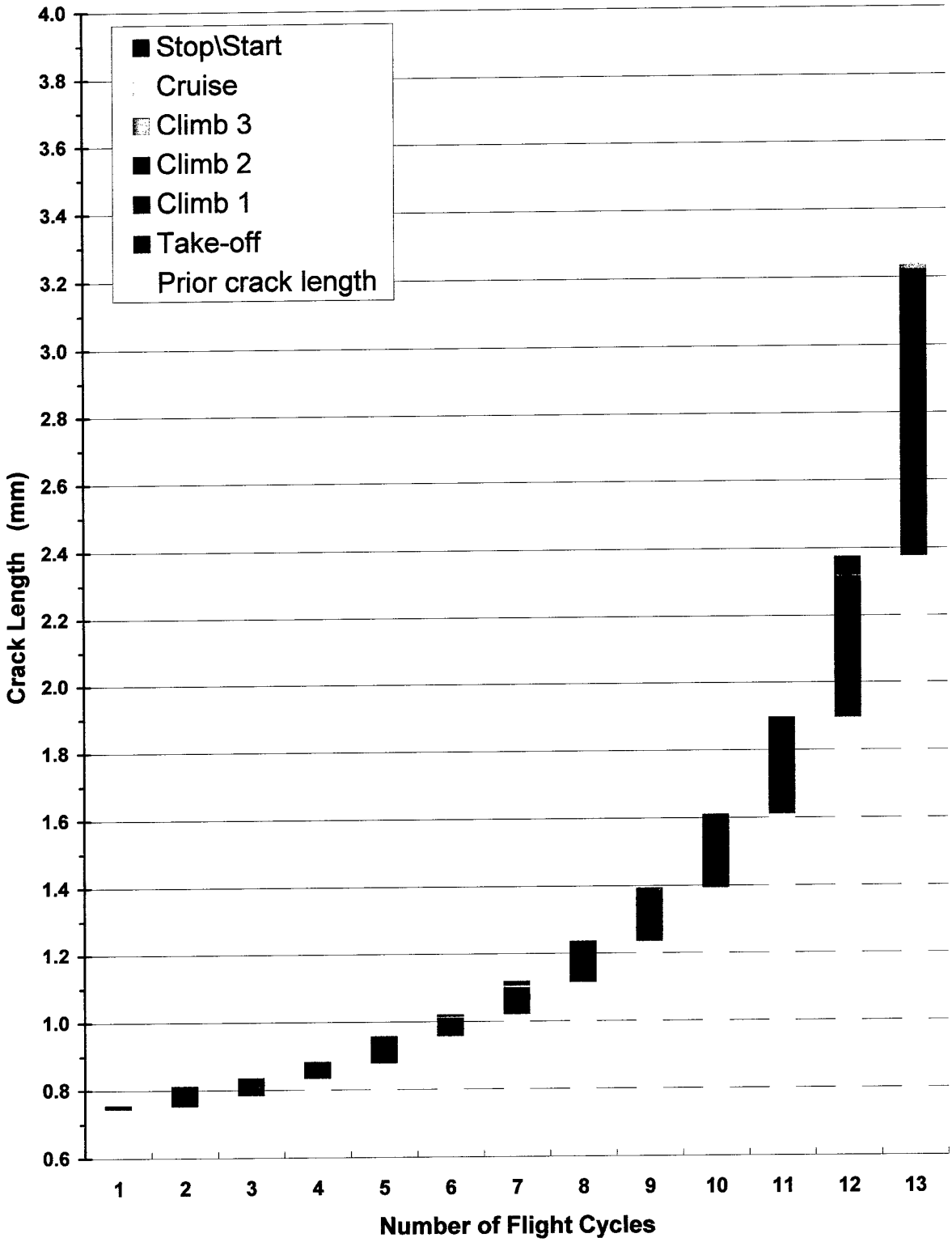

Figure 3 Contribution to crack growth by each stage of the flight simulation following the onset of combined loading effects. Test 1.

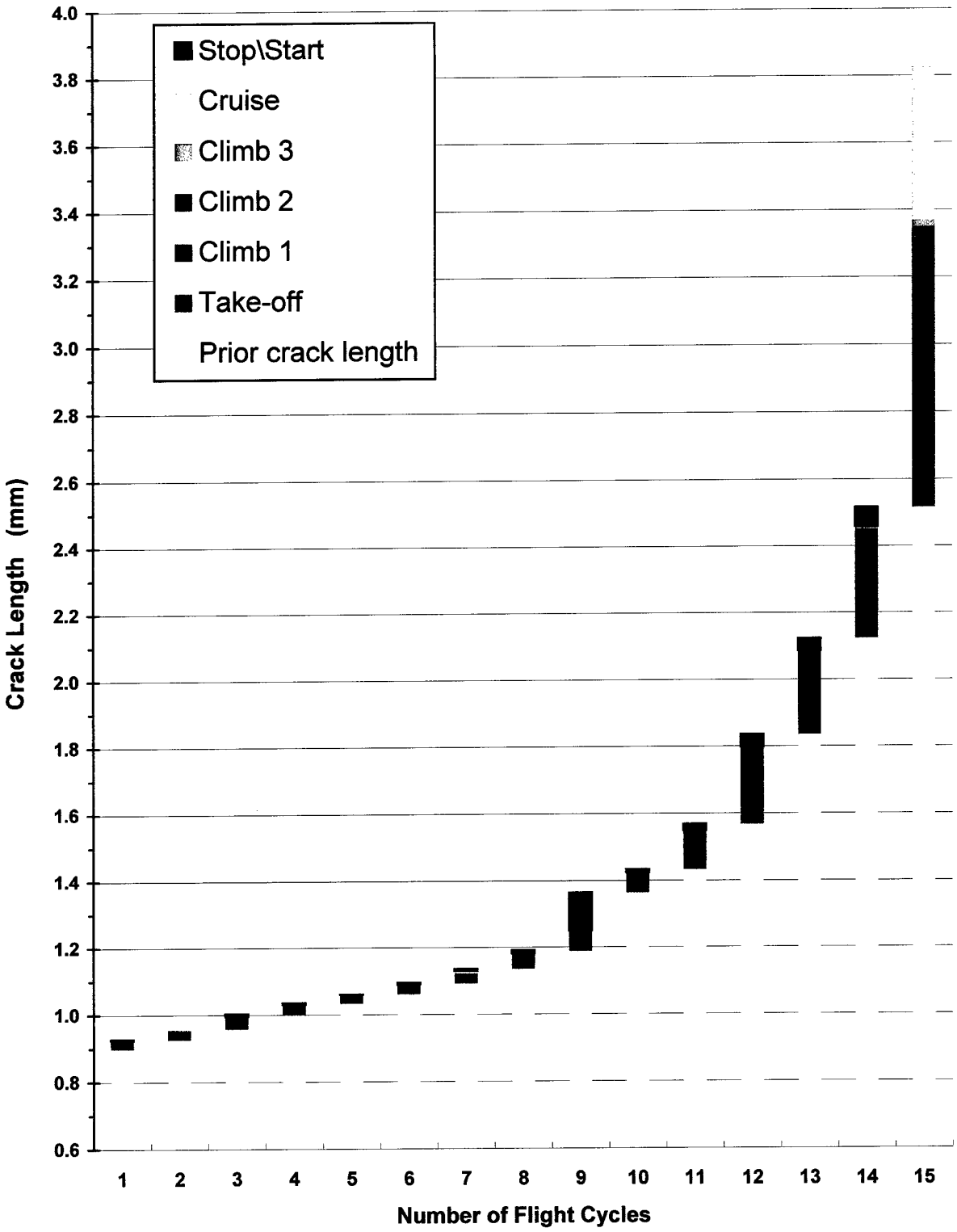

Figure 4 Contribution to crack growth by each stage of the flight simulation following the onset of combined loading effects, Test 2.

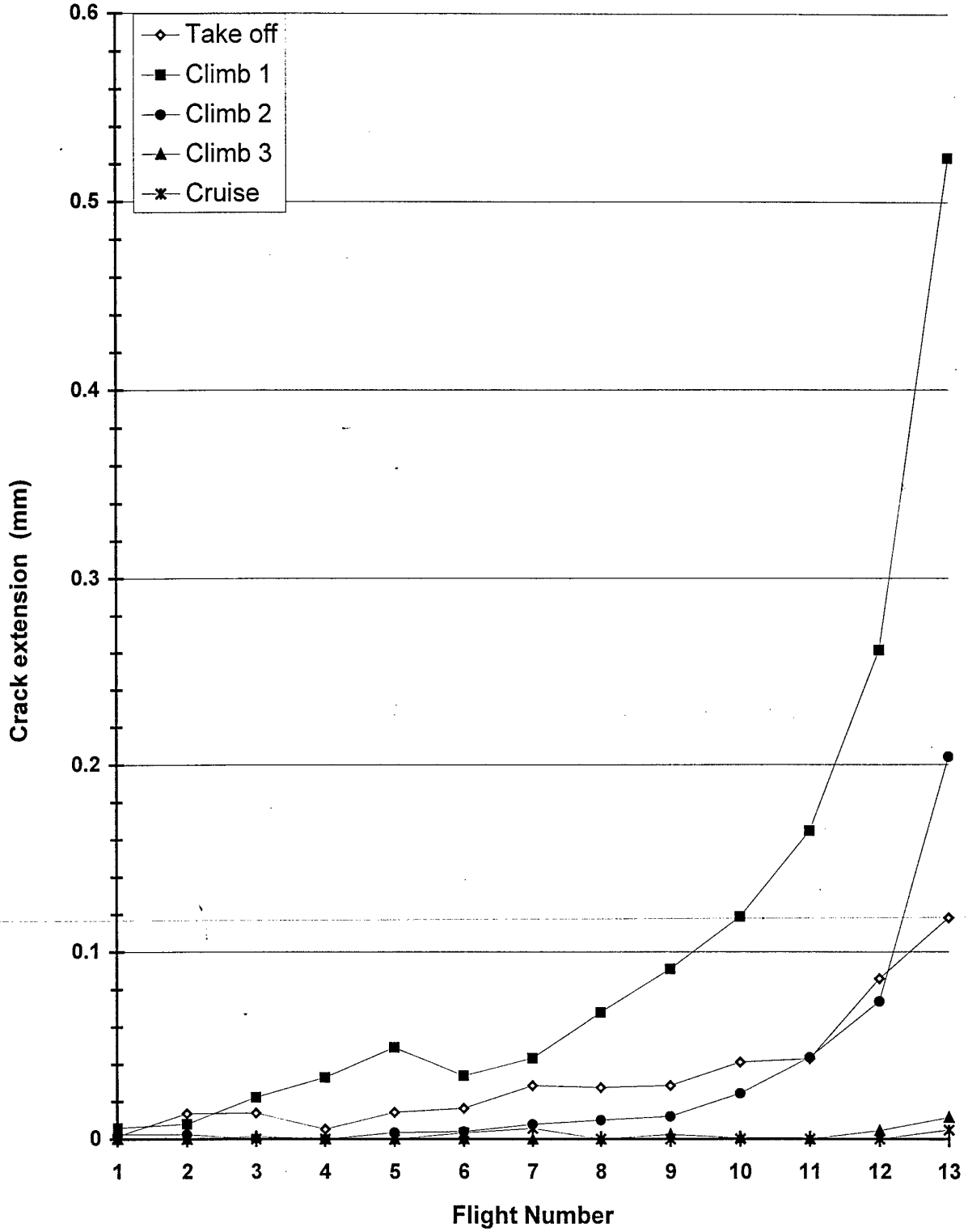

Figure 5 Crack extension at each stage of the flight cycle following the onset of combined loading effects. Test 1.

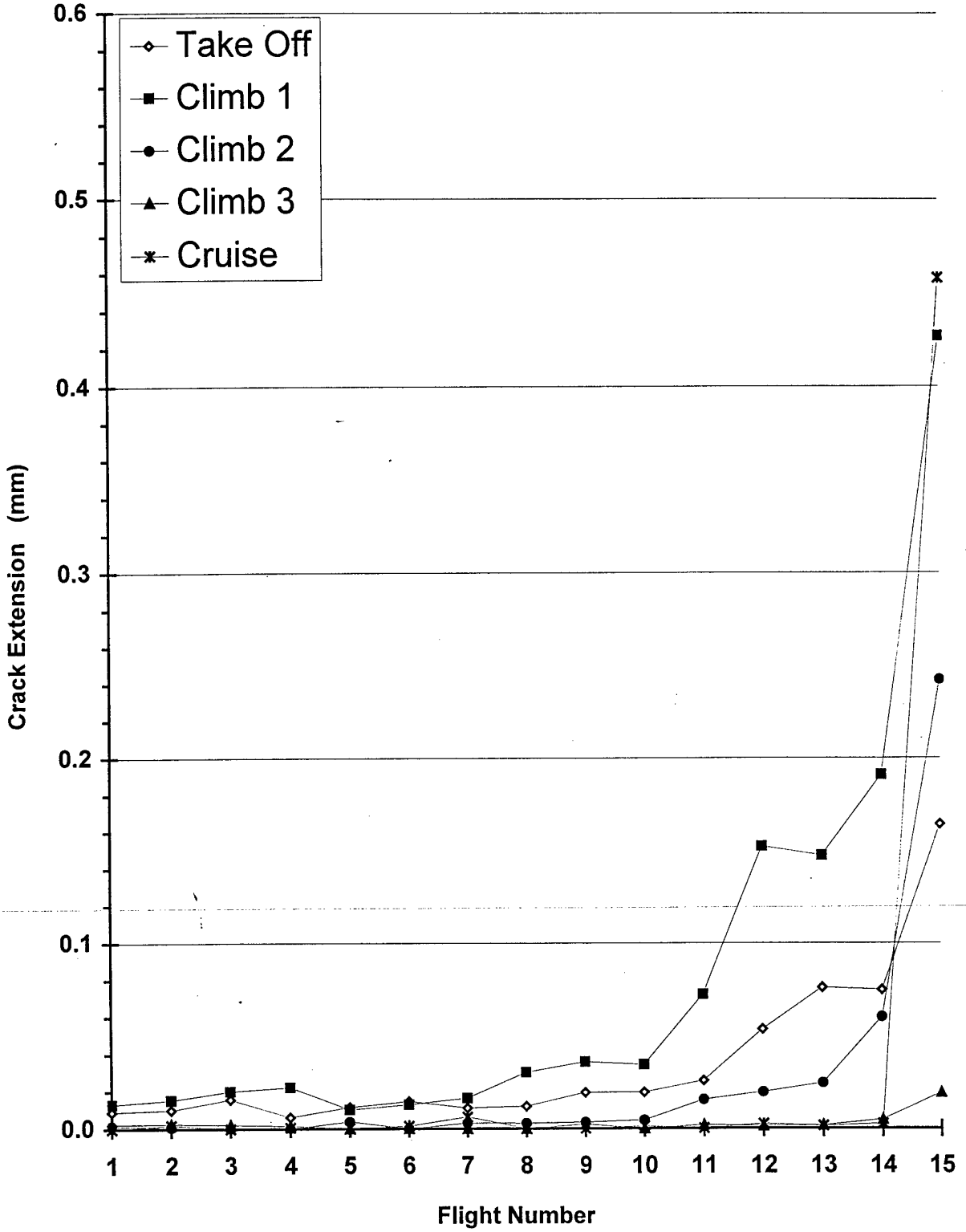

Figure 6 Crack extension at each stage of the flight cycle following the onset of combined loading effects, Test 2.

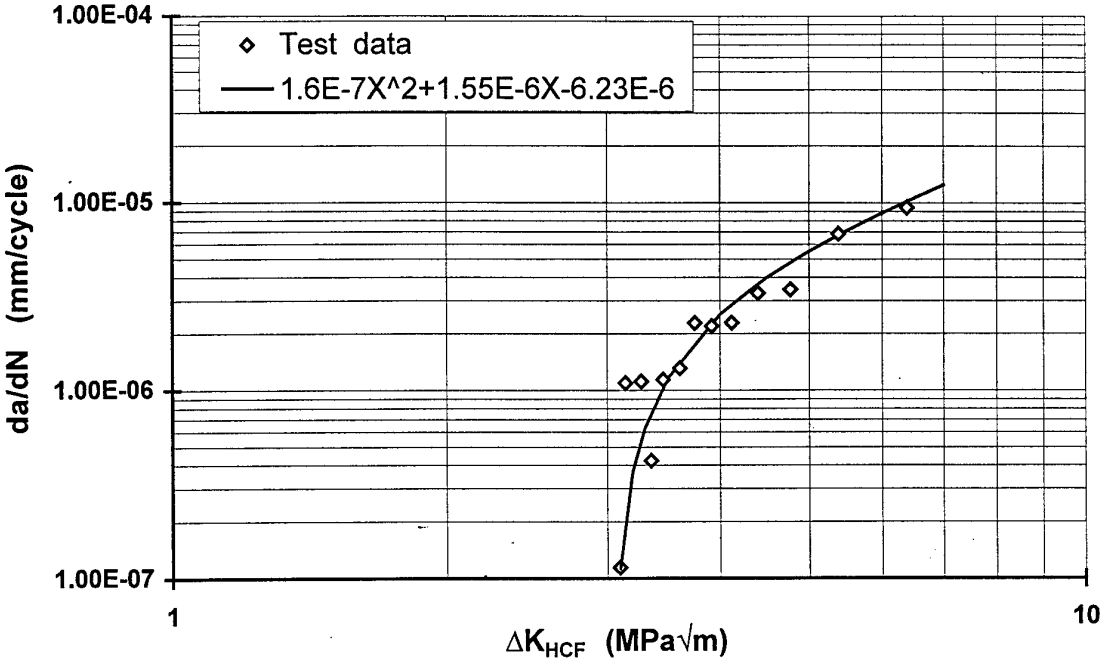

Figure 7a Test 1.

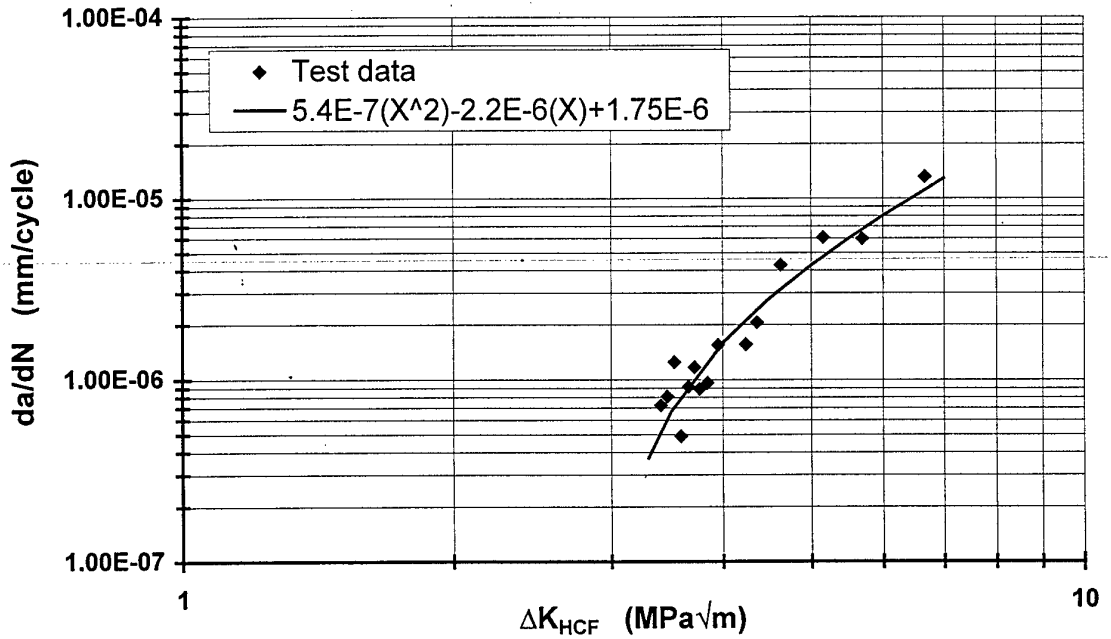

Figure 7b Test 2

FCG rates from TAKE OFF stage of flight cycles, with fitted polynomial curve.

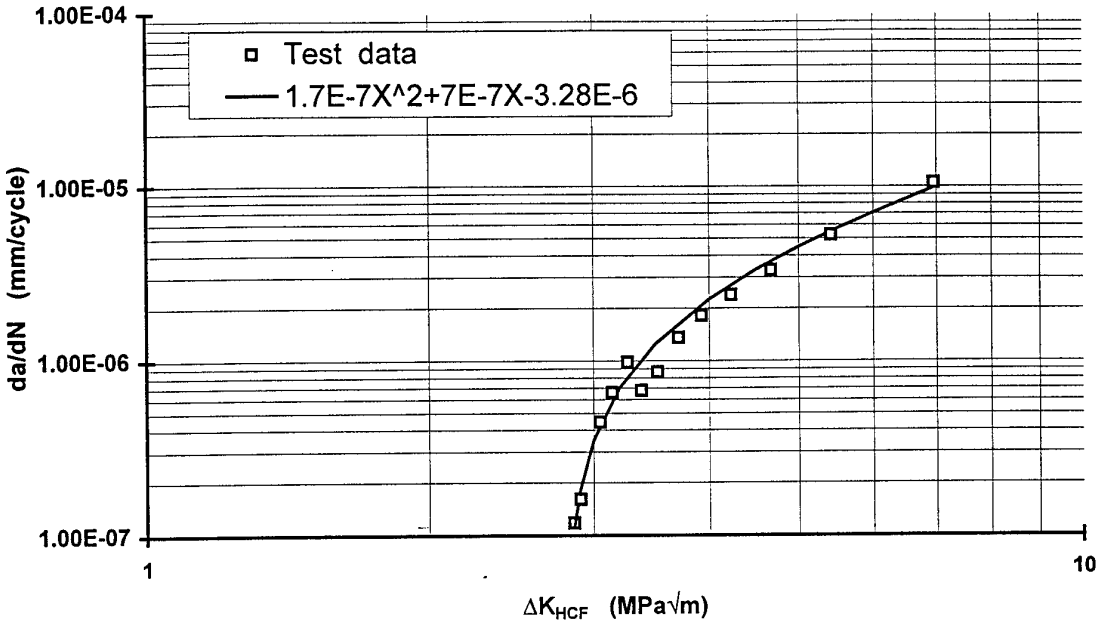

Figure 8a Test 1.

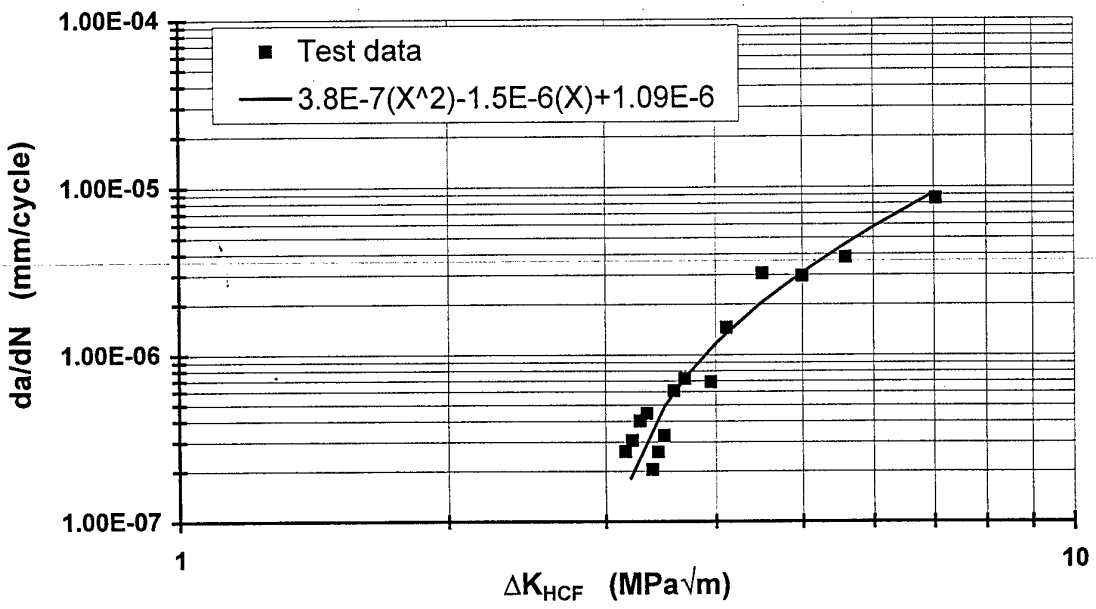

Figure 8b Test 2.

FCG rates from CLIMB 1 stage of flight cycles, with fitted polynomial curve

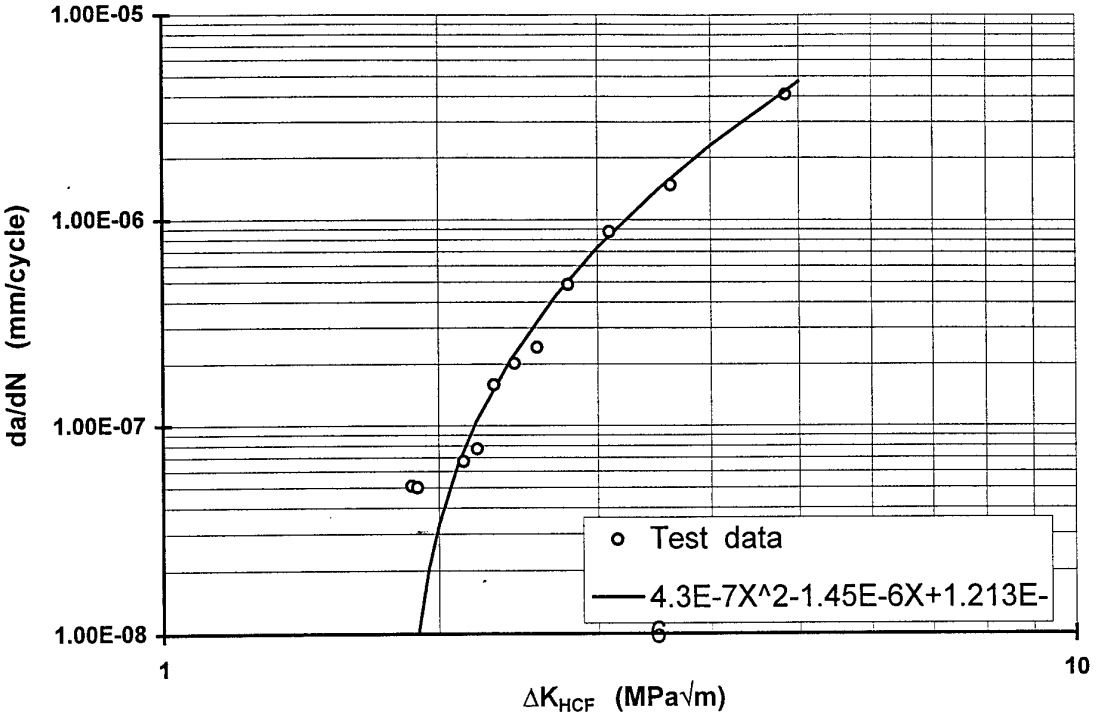

Figure 9a Test 1.

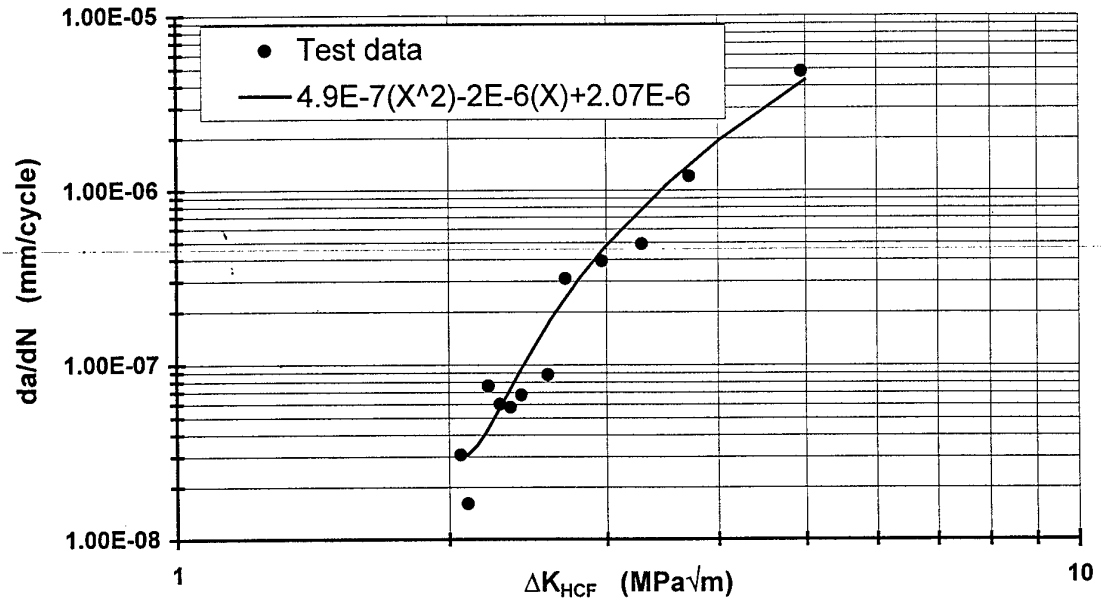

Figure 9b Test 2.

FCG rates from CLIMB 2 stage of flight cycles, with fitted polynomial curve

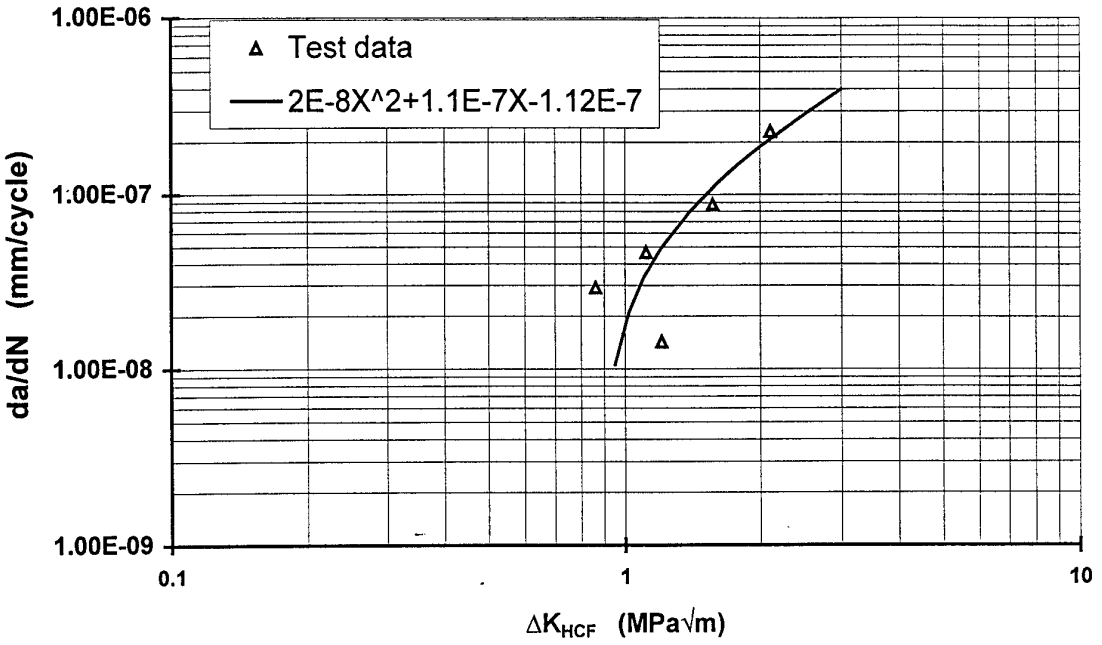

Figure 10a Test 1.

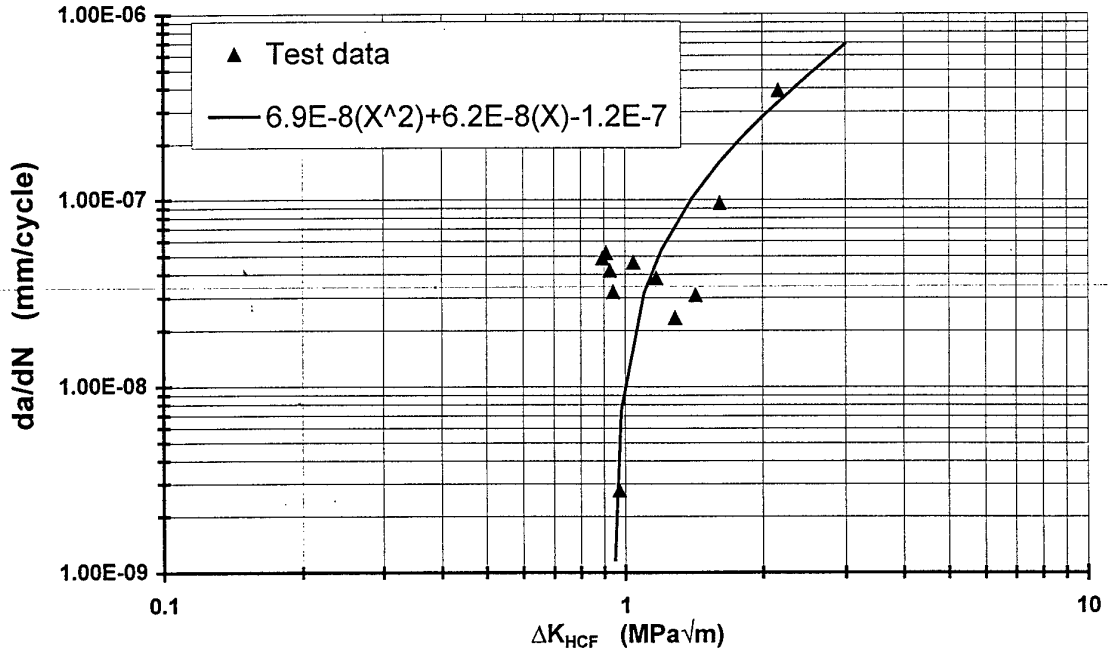

Figure 10b Test 2.

FCG rates from CLIMB 3 stage of flight cycles, with fitted polynomial curve

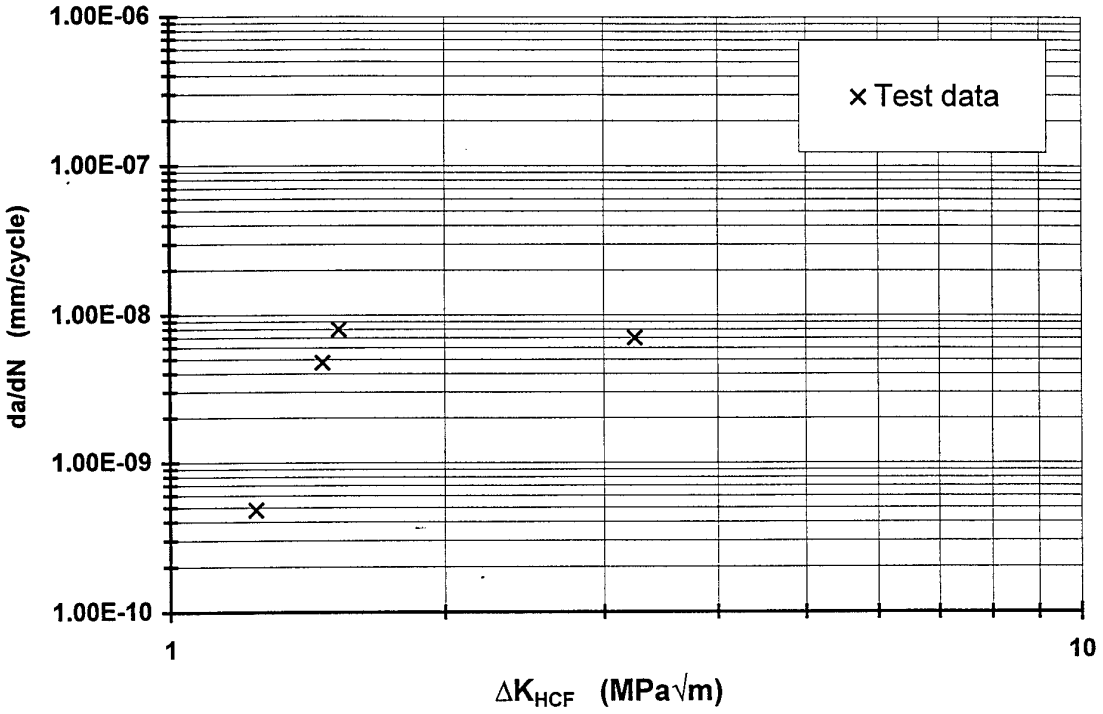

Fugure 11a Test 1.

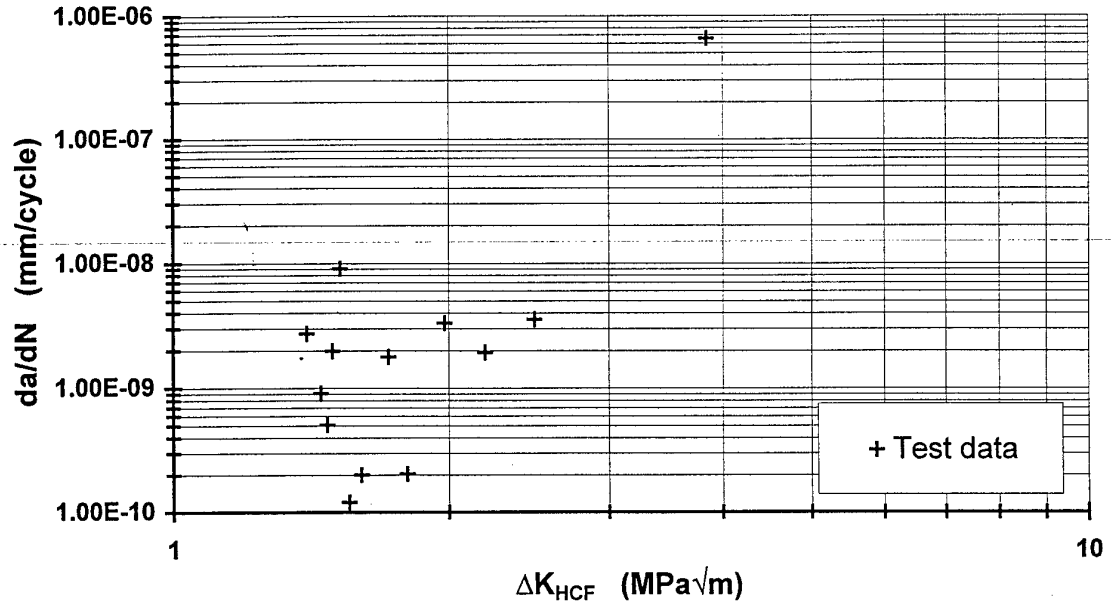

Figure 11b Test 2.

FCG rates from CRUISE stage of flight cycles, with fitted polynomial curve

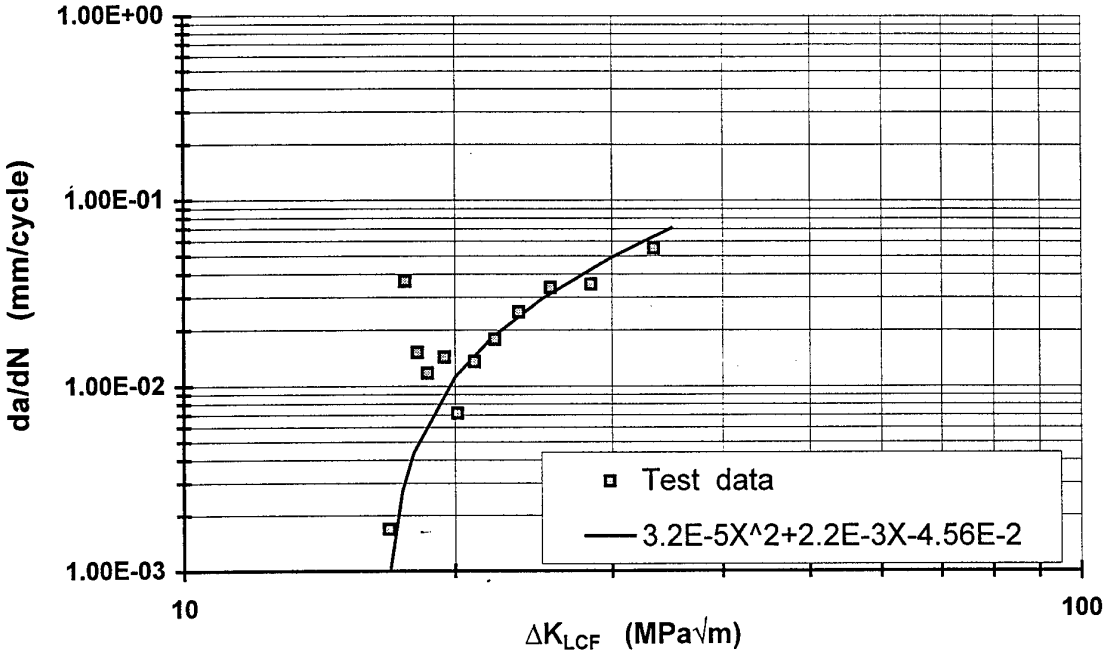

Figure 12a Test 1.

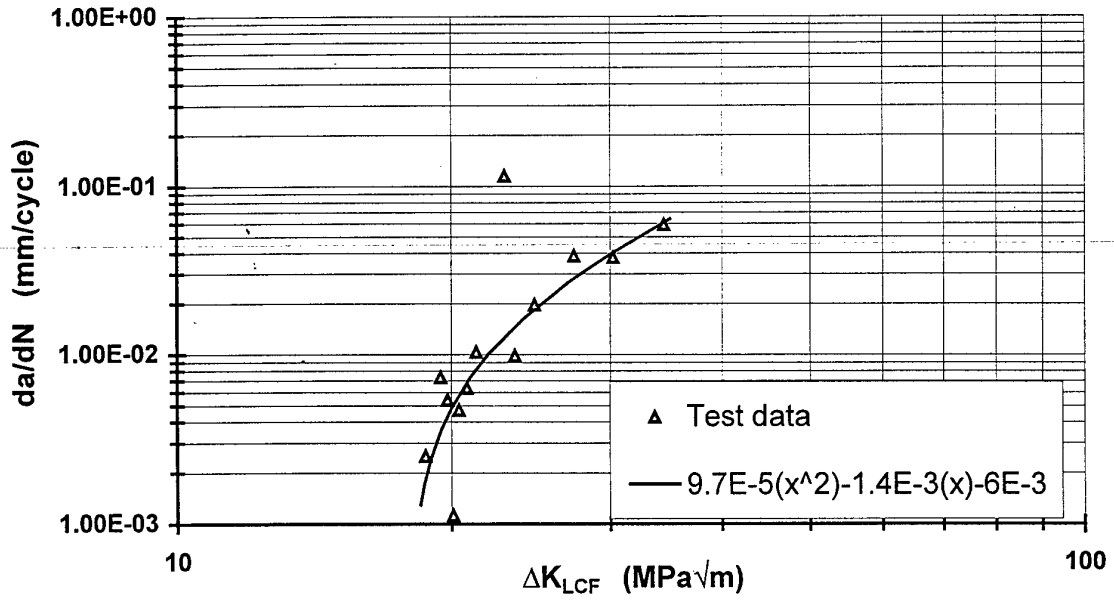

Figure 12b Test 2.

FCG rates from STOP/START stage of flight cycles, with fitted polynomial curve

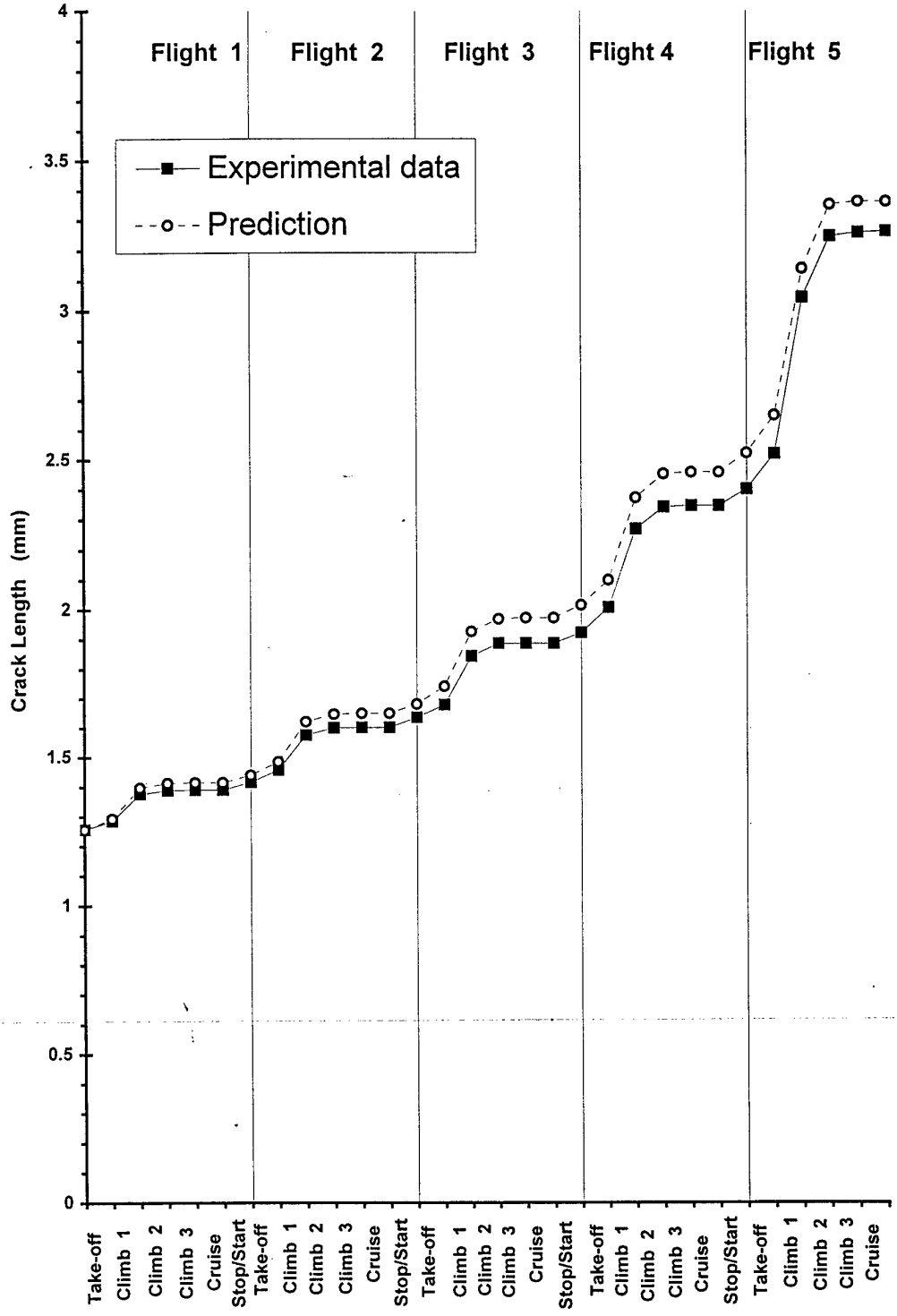

Figure 13 Comparison of crack length from experimental data against predictions based on polynomial curves for FCG during individual stages of the final 5 flights in test 1

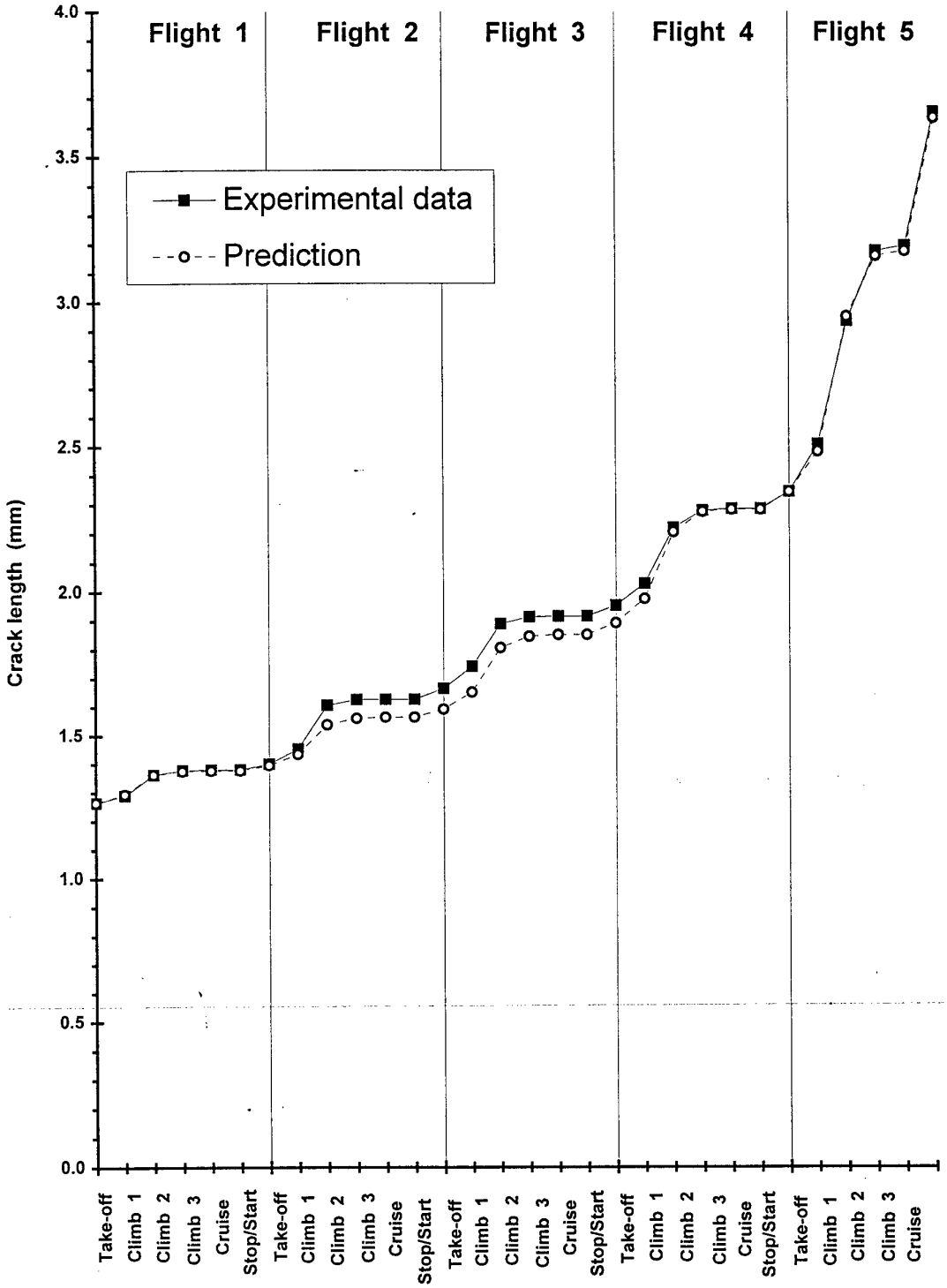

Figure 14 Comparison of crack length from experimental data against predictions based on polynomial curves for FCG during individual stages of the final 5 flights of test 2.

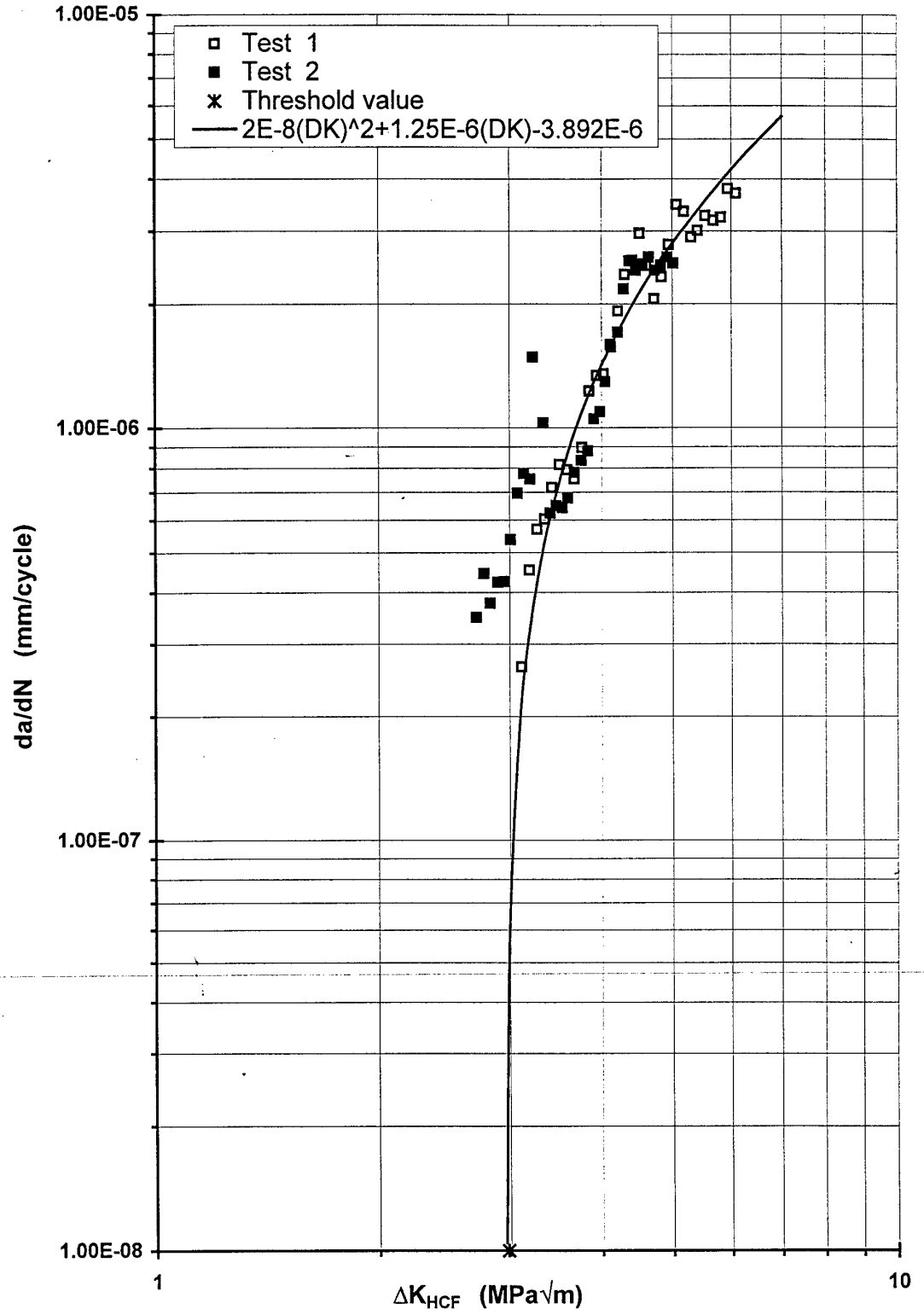

Figure 15 Near-threshold FCG rates for HCF cycles at R_{HCF} = 0.7. Results from 2 tests.

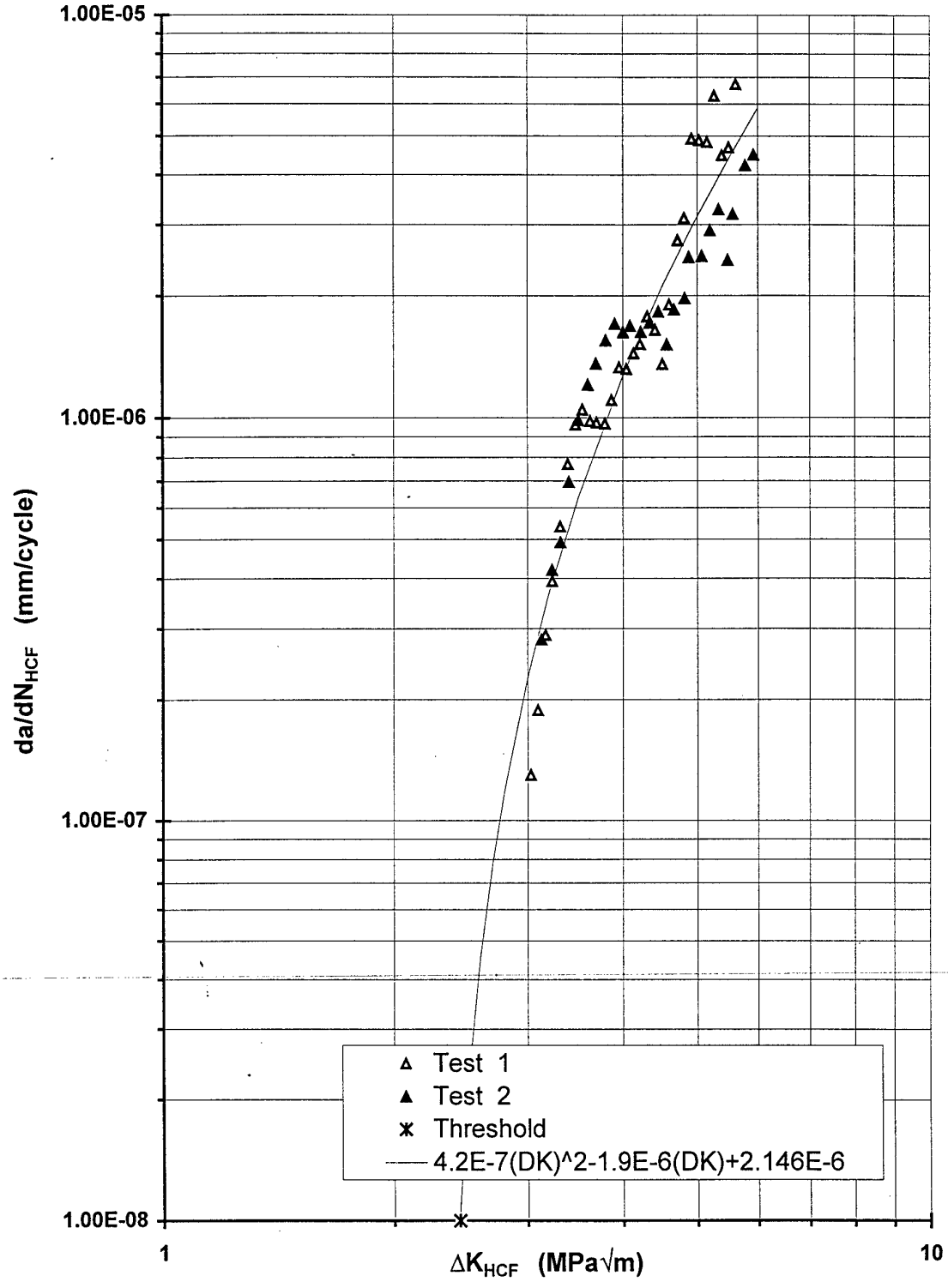

Figure 16 Near-threshold FCG rates for HCF cycles at R_{HCF} = 0.8. Results from 2 tests.

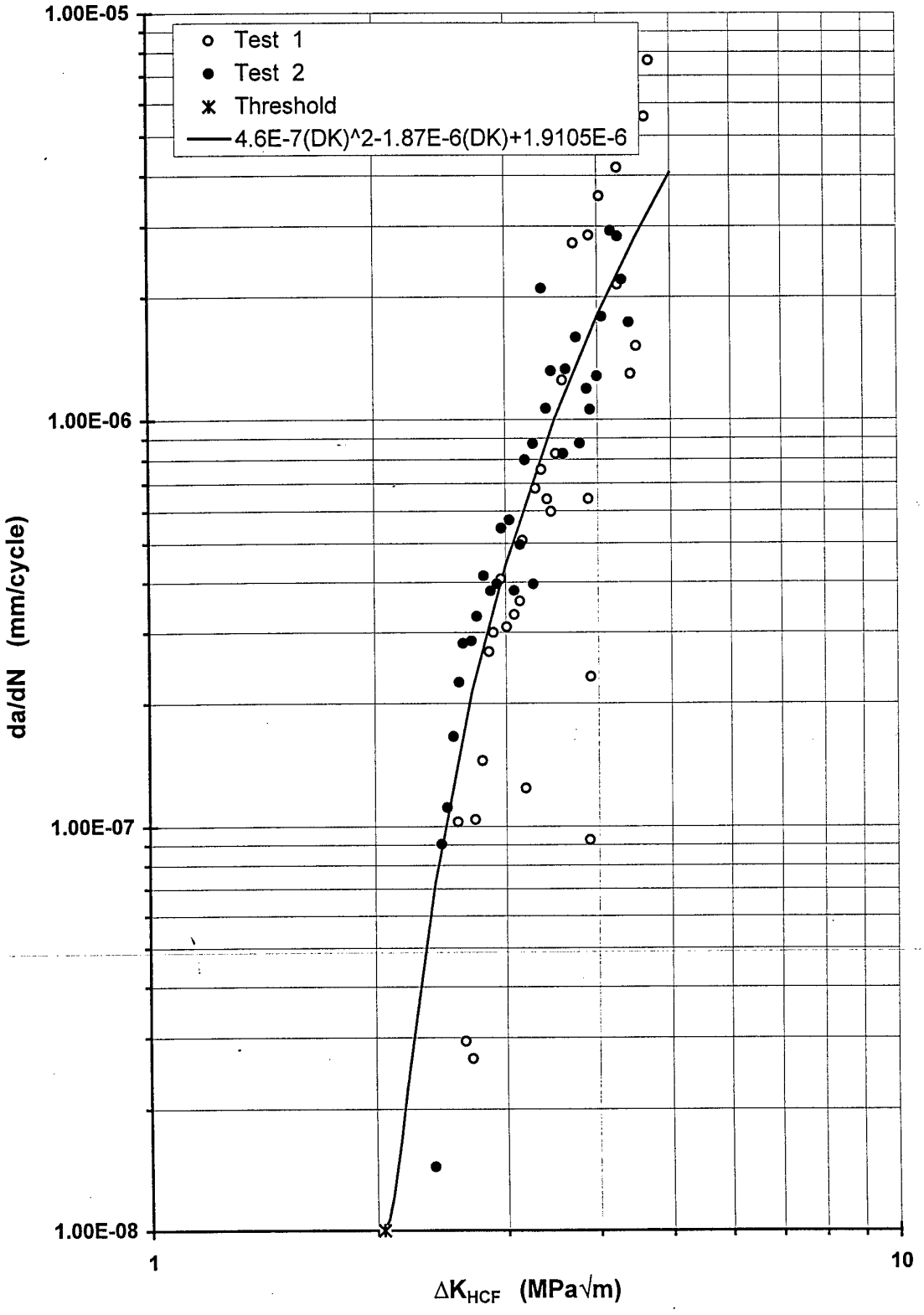

Figure 17 Near-threshold FCG rates for HCF cycles at R_{HCF} = 0.9. Results from 2 tests.

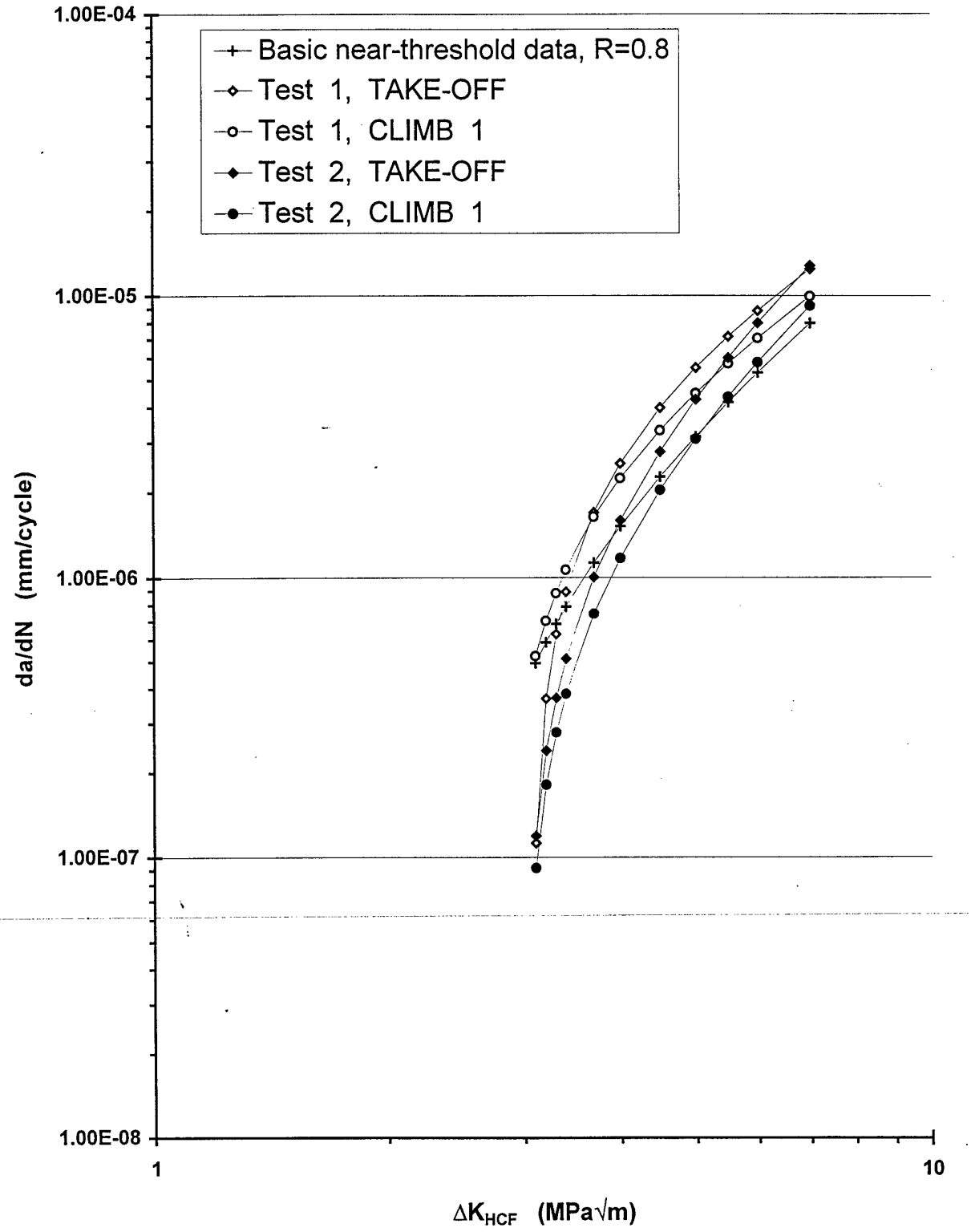

Figure 18 Comparison of FCG rates for basic HCF data for near-threshold with TAKE-OFF and CLIMB 1 stages of flight

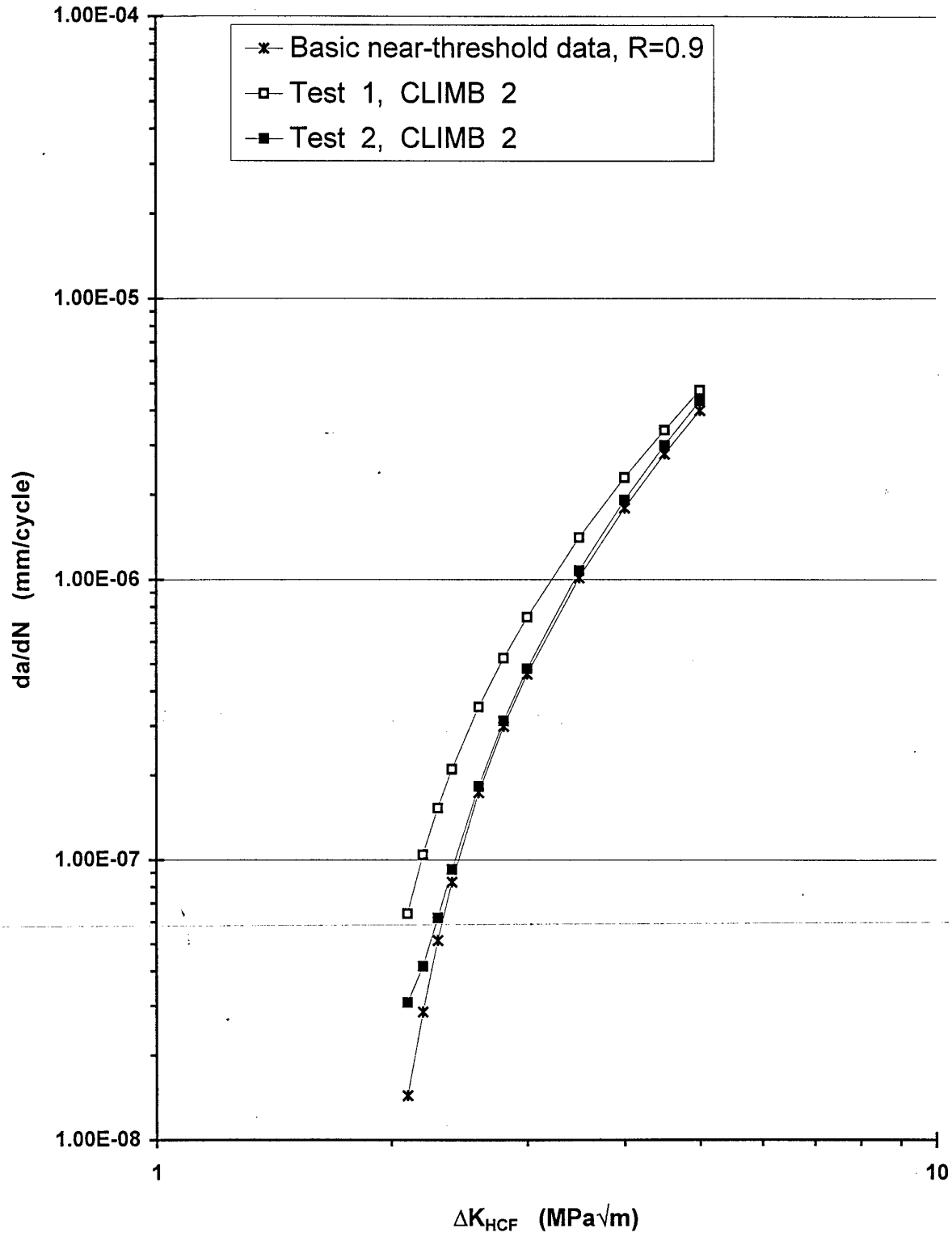

Figure 19 Comparison of FCG rates for basic HCF data for near-threshold with CLIMB 2 stage of flight

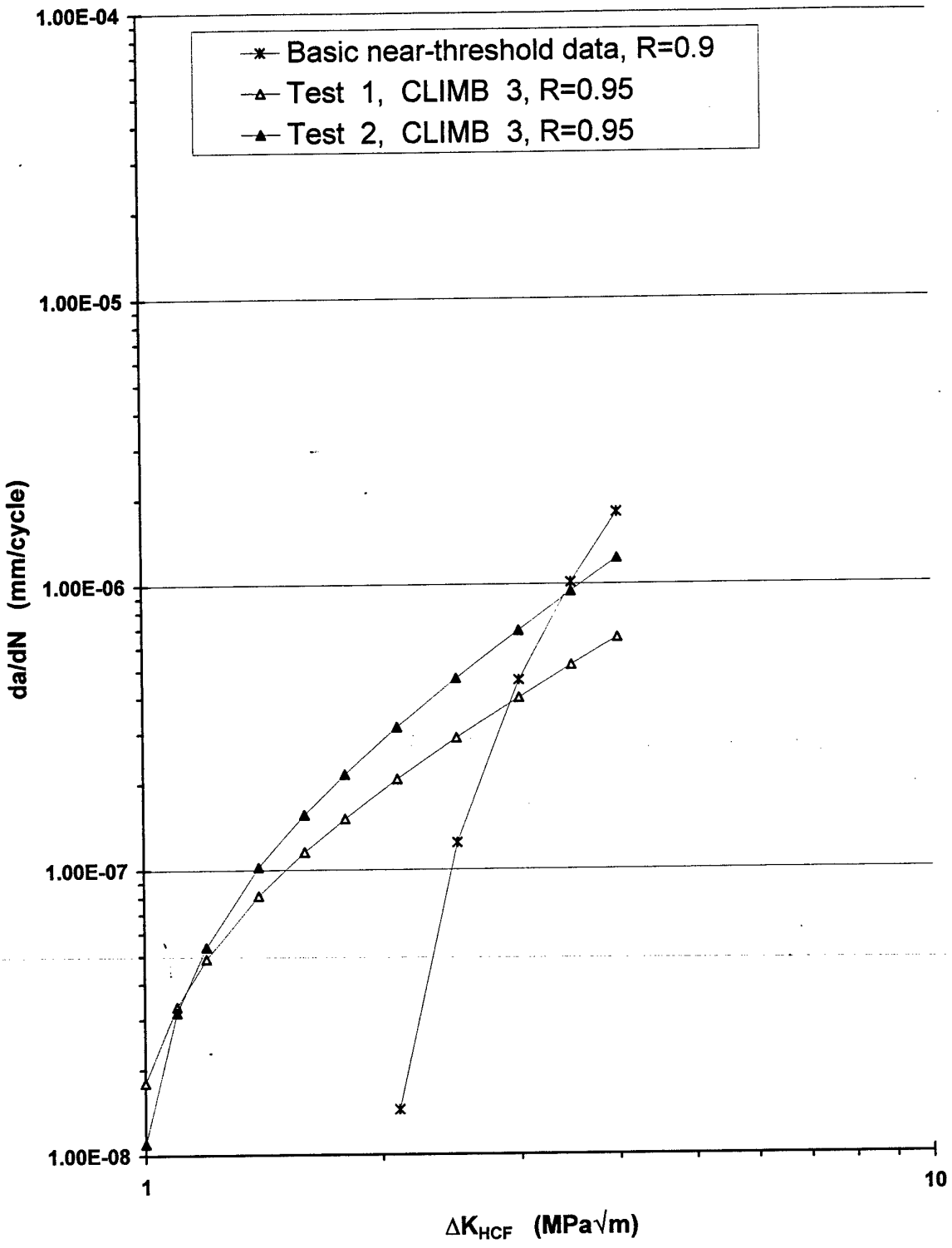

Figure 20 Comparison of FCG rates for basic HCF data for near-threshold with CLIMB 3 stage of flight